Remote Sensing of Environment 115 (2011) 3343–3354

Contents lists available at ScienceDirect

Remote Sensing of Environment

journal homepage: www.elsevier.com/locate/rse

A proposed extension to the soil moisture and ocean salinity level 2 algorithm for mixed forest and moderate vegetation pixels

Rocco Panciera [a,*], Jeffrey P. Walker [b], Jetse Kalma [c], Edward Kim [d]

[a] Cooperative Research Centre for Spatial information, The University of Melbourne, Australia
[b] Department of Civil Engineering, Monash University, Australia
[c] School of Engineering, The University of Newcastle, Australia
[d] NASA Goddard Space Flight Center, USA

ARTICLE INFO

Article history:
Received 4 April 2011
Received in revised form 26 July 2011
Accepted 30 July 2011
Available online 23 August 2011

Keywords:
SMOS
SMOS Level 2
Passive microwave
Soil moisture
Spatial heterogeneity

ABSTRACT

The Soil Moisture and Ocean Salinity (SMOS) mission, launched in November 2009, provides global maps of soil moisture and ocean salinity by measuring the L-band (1.4 GHz) emission of the Earth's surface with a spatial resolution of 40–50 km. Uncertainty in the retrieval of soil moisture over large heterogeneous areas such as SMOS pixels is expected, due to the non-linearity of the relationship between soil moisture and the microwave emission. The current baseline soil moisture retrieval algorithm adopted by SMOS and implemented in the SMOS Level 2 (SMOS L2) processor partially accounts for the sub-pixel heterogeneity of the land surface, by modelling the individual contributions of different pixel fractions to the overall pixel emission. This retrieval approach is tested in this study using airborne L-band data over an area the size of a SMOS pixel characterised by a mix Eucalypt forest and moderate vegetation types (grassland and crops), with the objective of assessing its ability to correct for the soil moisture retrieval error induced by the land surface heterogeneity. A preliminary analysis using a traditional uniform pixel retrieval approach shows that the sub-pixel heterogeneity of land cover type causes significant errors in soil moisture retrieval (7.7%v/v RMSE, 2%v/v bias) in pixels characterised by a significant amount of forest (40–60%). Although the retrieval approach adopted by SMOS partially reduces this error, it is affected by errors beyond the SMOS target accuracy, presenting in particular a strong dry bias when a fraction of the pixel is occupied by forest (4.1%v/v RMSE, −3.1%v/v bias). An extension to the SMOS approach is proposed that accounts for the heterogeneity of vegetation optical depth within the SMOS pixel. The proposed approach is shown to significantly reduce the error in retrieved soil moisture (2.8%v/v RMSE, −0.3%v/v bias) in pixels characterised by a critical amount of forest (40–60%), at the limited cost of only a crude estimate of the optical depth of the forested area (better than 35% uncertainty). This study makes use of an unprecedented data set of airborne L-band observations and ground supporting data from the National Airborne Field Experiment 2005 (NAFE'05), which allowed accurate characterisation of the land surface heterogeneity over an area equivalent in size to a SMOS pixel.

1. Introduction

Frequent and global soil moisture observations are crucial to many environmental disciplines such as flood forecasting (Western et al., 2004), improved modelling of erosion-affected lands (Castillo et al., 2003), weather and climate forecasting (Conil et al., 2007; Koster et al., 2003), and agricultural applications (Bolten et al., 2010). The first satellite mission specifically designed for remote sensing of near-surface soil moisture is the Soil Moisture and Ocean Salinity (SMOS) mission from the European Space Agency (ESA), succesfully launched on November 2, 2009. SMOS carries an L-band (1.4 GHz) 2D interferometric radiometer that provides near-surface soil moisture estimates with global coverage, a revisit time of three days and spatial resolution of 40–50 km (depending on the position within the field-of-view). The SMOS target accuracy is 4%v/v, which should be achievable over relatively uniform areas with vegetation water content up to approximately 5 kg/m^2, outside mountainous, urban, and partially frozen or snow covered areas (CESBIO, 2011; Jackson et al., 1999; Panciera et al., 2009a; Uitdewilligen et al., 2003).

Soil moisture is generally retrieved from L-band observation by inversion of a radiative transfer model which simulates the emission of the Earth's surface under the assumption of spatial homogeneity within the remote sensor footprint ("uniform pixel" approach). However, the heterogeneity in surface conditions within SMOS footprints (40–50 km) will obviously be significant. Since the coupling of radiation from different surface components into the sensor receiving aperture, as expressed by the radiative transfer and sensor response equations, is nonlinear, errors may occur in the retrieval of soil moisture at the scale

* Corresponding author at: CRC for Spatial Information, PO Box 672, Carlton South VIC 3053, Australia. Tel.: +61 3 83445628; fax: +61 3 9654 6515.
E-mail address: panr@unimelb.edu.au (R. Panciera).

0034-4257/$ – see front matter © 2011 Elsevier Inc. All rights reserved.
doi:10.1016/j.rse.2011.07.017

of SMOS pixels if these heterogeneities are not accounted for. Several studies have investigated the effect of heterogeneity of individual land surface factors (soil moisture, texture and temperature and vegetation water content) on soil moisture retrieval from passive microwave observations using analytical analyses. These studies have indicated that heterogeneity in soil moisture, soil texture and soil temperature results in soil moisture errors comparable to the instrument noise of a typical radiometer (Davenport et al., 2008; Galantowicz et al., 2000; Njoku et al., 1996). However, the effect of heterogeneity in Vegetation Water Content (VWC) was found to be significant (Bindlish & Barros, 2002; Van de Griend et al., 2003), with errors as high as 12%v/v volumetric soil moisture in the worst case of cold, wet soil (Bindlish & Barros, 2002; Burke & Simmonds, 2003), increasing exponentially with the degree of VWC heterogeneity (Burke et al., 2004). A limited number of studies based on coarse-resolution (up to 800 m) airborne data sets collected during the Washita'92, Southern Great Plains'97 and '99 analysed the effect of land surface heterogeneity on soil moisture retrieval using real L-band observations, generally observing that the radiative transfer parameters of the retrieval algorithms developed with tower-based radiometers needed to be adjusted for coarse pixels, implicitly incorporating the effect of land surface heterogeneity. (Drusch et al., 1999; Guha & Lakshmi, 2002; Jackson, 2001; Jackson et al., 1999).

To compensate for the effect of sub-pixel heterogeneity, a novel retrieval approach has been adopted for the SMOS mission and implemented in the SMOS L2 processor (CESBIO, 2011). The approach, hereby referred to as simply the "SMOS approach", is based on the physically-based method proposed by Kerr and Njoku (1993) and Njoku et al. (1996), and consists of modelling the microwave emission from different pixel fractions of the heterogeneous pixel, which are then aggregated (using areal weighting) to compute the pixel emission. The method, as implemented in SMOS, relies on the assumption that land cover is the main source of land surface variability affecting the soil moisture retrieval. Moreover, in the presence of only "moderate" canopy conditions (such as crops and grasslands) and forest with a density below a defined threshold, the assumption is made that the retrieved parameters (i.e., soil moisture alone, or both soil moisture and optical depth) are uniform amongst different scene components (i.e., have the same value for each land cover fraction within the pixel).

Despite its adoption by the SMOS mission, the approach has thus far received little consideration in literature. Drusch et al. (1999) tested the core concept of fractional coverage with the SGP'97 airborne data set. However, the method as applied in that study only considered a limited number of cases, these being pixels with 100% vegetation cover and pixels with 80% vegetation cover/20% bare soil, which do not represent the large variety of real-world conditions. Moreover, the vegetated fraction was comprised of mostly low-density vegetation, i.e., mainly rangeland and pasture with some areas of crops. Consequently, this study tests the SMOS approach and its efficacy in compensating for land surface heterogeneity using an airborne data set that covers a variety of land surface conditions including a mix of grasslands, crops and Eucalypt forests. The unique data set used comprises the airborne L-band observations and ground soil moisture and ancillary data (vegetation, soil temperature, soil texture and surface roughness) collected during the National Airborne Field Experiment 2005 (NAFE'05) in the Goulburn catchment, south-eastern Australia (Panciera et al., 2008). The extent and detail of ground monitoring performed during NAFE'05 across an entire SMOS pixel makes this an unprecedented data set to analyse the effect of land surface heterogeneity on SMOS soil moisture retrieval.

2. Data and methodology

The analysis presented in this paper is divided into three phases. First, the airborne and ground data from the NAFE'05 experiment are processed to create coarse-resolution pixels and high resolution soil moisture maps; the latter are used as validation data to assess the performance of the soil moisture retrieval at coarse scale. Phase two uses a traditional two-channel uniform pixel retrieval scheme to retrieve soil moisture from the coarse observations produced in phase one, in order to identify the land suface factors whose heterogeneity have the greatest impact on the soil moisture retrieval and to quantify the error in soil moisture retrieval induced by such heterogeneity. The third phase tests a proposed extension to the SMOS L2 approach.

Coarse-resolution brightness temperature (T_B) observations were produced in this study by aggregation of air-borne observations collected at 1 km resolution on 4 dates across a 40 km × 40 km area during the NAFE'05 experiment. The soil moisture retrieved from coarse-resolution observations using the three approaches are compared with validation data sets composed of high-resolution (1 km) resolution soil moisture maps of the study area, derived from the 1 km resolution air-borne T_B observations. In order to analyse a variety of retrieval scenarios over different land surface heterogeneity conditions, which would have be limited if only the 40 km observations of a single SMOS pixel were considered, the analysis was additionally conducted at various intermediate resolutions (5 km, 10 km, 20 km and 30 km). The airborne product used for validation had been previously verified over eight experimental sites with ground soil moisture measurements collected over nested grids at spacing from 6.25 to 1 km, yielding an estimated accuracy better than 4.8%v/v for crops and grasslands and 6%v/v over the Eucalypt forest (Panciera et al., 2009a).

2.1. Experiment description

The National Airborne Field Experiment 2005 (NAFE'05) took place between October 31 and November 25 in the Goulburn River catchment, located in south-eastern Australia (see Fig. 1). The aircraft and ground operations were concentrated on a 40km × 40 km study area in the northern part of the catchment, chosen for its moderate vegetation cover, including crops (mainly wheat and barley), grassland pasture and a limited area of Eucalypt forest, and the presence of numerous soil moisture monitoring sites (see Fig. 1). Airborne passive microwave and concurrent ground data on soil moisture, vegetation and surface roughness were collected on 18 dates. Heavy rainfalls on October 30 and 31 followed by a dry period allowed observations across the full range of soil moisture conditions, with the average soil moisture measured at the continuous monitoring sites decreasing from 47.9%v/v to 11.0%v/v during the experiment. In this section the NAFE'05 data relevant to this study are briefly introduced. Full details on the data set, including a description of the NAFE'05 study region, the airborne and ground instruments, and the data sets can be found in Panciera et al. (2008) and Panciera et al. (2009a).

2.1.1. Airborne data

Airborne data were collected using the Polarimetric L-band Multibeam Radiometer (PLMR). The PLMR is a dual polarised L-band radiometer which measures both V and H polarised brightness temperatures (T_B) at six incidence angles (7°, 21.5° and 38.5° from nadir on both sides of the aircraft) when flying in push-broom configuration. The accuracy of PLMR, derived from daily calibration during the experiment, was estimated to be better than 1 K (H polarisation) and 2.5 K (V polarisation) (Panciera, 2009). The data used in this study to produce coarse-scale SMOS observations were PLMR observations at 1 km resolution collected from 3,000 m flying height over the entire 40 km × 40 km study area on four consecutive days a week apart ("Regional flights", October 31, November 7, 14 and 21). All flights were performed between approximately 7:00 AM and 9:30 AM so as to closely simulate the SMOS overpass time (6:00 AM) whilst also minimising the possible complications from dew on the vegetation, which might be significant over some vegetation canopies

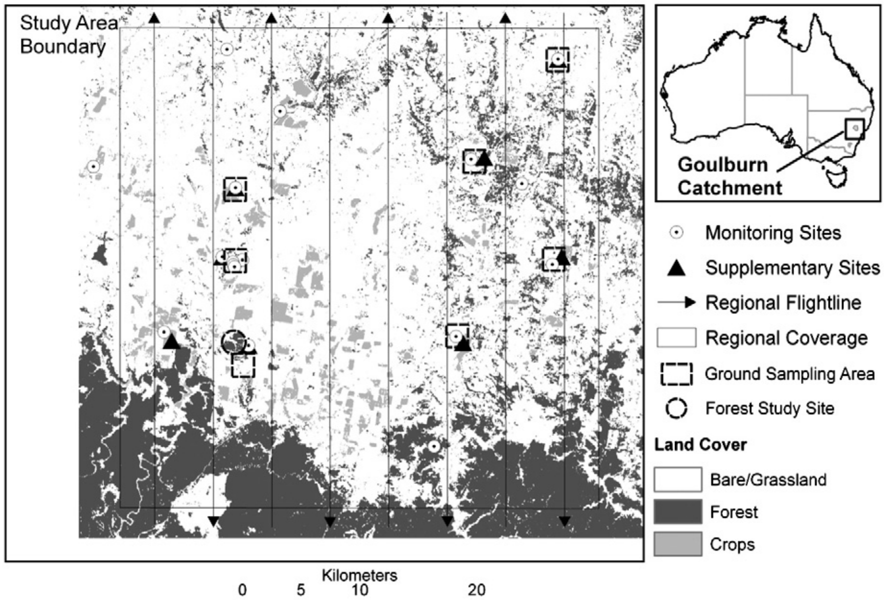

Fig. 1. Flightlines, ground validation sites and continuous monitoring sites in the NAFE'05 study area, with land cover map derived from Landsat 5 as background.

(Saleh et al., 2006). The airborne observations were geo-located using aircraft position and attitude information and taking into account topography through a Digital Elevation Model (DEM) of the study area.

Prior to gridding to a 1 km reference grid, the T_B observations were processed to eliminate changes in emissivity due to incidence angle differences and temporal changes of soil temperature during the flight, which are undesirable when performing soil moisture retrieval over large areas. The variation in incidence angle was accounted for using a procedure proposed by Jackson (2001) which uses beam-specific correction factors based on the daily average T_B for each beam. Using this procedure, the regional T_B observations were normalised to the incidence angle of the radiometer's outermost beams (38.5°). This angle was chosen so as to maximise the retrieval accuracy of L-MEB, which has been shown to be higher at off-nadir angles (Wigneron et al., 2000), and also because it is very close to the viewing configuration of the radiometer of the future Soil Moisture Active Passive (SMAP) mission, extending the relevance of the results presented in this study. To compensate for the temporal variation of the surface temperature during the Regional flights (up to 2.6 K change at 2.5 cm depth between 7:00 and 9:30 AM) the airborne T_B observations were normalised to an intermediate reference time (8:00 AM) using the surface temperature data from the monitoring sites. The soil temperature used in the soil moisture retrieval was then taken as the average soil temperature between the monitoring sites at the reference time (8:00 AM).

Coarse-resolution T_B observations at 38° incidence angle were produced by aggregating the T_B observations collected during the Regional flights to 5, 10, 20, 30, and 40 km resolutions using a "moving window" approach. This involved averaging the 1 km T_B's falling within "windows" at each of the resolutions indicated above, which were moved around the study area in order to increase the sample size. This technique was chosen to allow the analysis of a much wider variety of conditions of land surface heterogeneity than is possible with pixels at 40 km resolution (i.e., uniform pixels as well as heterogeneous pixels, and heterogeneity of different land surface factors). The total number of coarse pixels produced was respectively 256, 196, 100, 36 and 4 (over four dates). The reliability of linear aggregation of high-resolution airborne observations to produce realistic coarse-scale T_B observations was verified by a previous study by Panciera et al. (2007) using the NAFE'05 multi-resolution flights, confirming independent analysis by Jackson (2001).

2.1.2. Ground monitoring

Continuous ground observations of rainfall, soil moisture profiles (0 m–90 cm) and near-surface temperature (2.5 cm and 15 cm) were provided by eighteen permanent sites, together with continuous soil temperature (1, 2.5, 4 cm) at eight supplementary sites, four of which had thermal infrared sensors for canopy temperature (see Fig. 1). Detailed ground sampling of soil moisture and vegetation properties was undertaken concurrently with all flights at 8 experimental farms. These data were used to validate the microwave emission model used in this study specifically for the study area (Panciera et al., 2009a). Soil moisture sampling was done using Stevens Water Hydraprobe dielectric probes, calibrated with over 120 gravimetric field samples yielding an estimated accuracy of ±3.5%v/v (Merlin et al., 2007).

2.2. L-MEB microwave model

The model used in this study, the L-band Microwave Emission of the Biosphere model, L-MEB, is the core of the SMOS mission retrieval algorithm ('SMOS Level 2'). L-MEB is the result of an extensive review of the current knowledge of microwave emission by various land covers and has been described in detail by Wigneron et al. (2007).

2.2.1. Model description

The emission from a vegetated soil surface is modelled in L-MEB using a 'τ–ω' approach with the above canopy brightness temperatures written as:

$$T_{BP}(\vartheta) = (1-\omega_P(\vartheta))(1-\gamma_P(\vartheta))(1+\Gamma_P(\vartheta)\gamma_P(\vartheta))T_V + (1-\Gamma_P(\vartheta))\gamma_P(\vartheta)T_{EFF}, \quad (1)$$

where the subscript p indicates the polarisation (Vertical or Horizontal) whilst ϑ is the incidence angle, ω the vegetation scattering albedo, γ_P is the transmissivity of the vegetation layer, Γ the soil microwave reflectivity, T_V the effective vegetation temperature and T_{EFF} the soil microwave effective temperature. The first right-hand term of Eq. (1) represents the direct vegetation emission and the vegetation emission reflected by the soil and attenuated by the canopy layer, whilst the second term accounts for the soil emission attenuated by the canopy.

The soil microwave emissivity is related to the reflectivity Γ as: $e_G = 1-\Gamma$. This is related to the soil dielectric constant (ε_G) through the Fresnel equations. The dependence of ε_G on soil moisture content for a specific soil type is accounted for using a dielectric mixing model. In this study, the same dielectric mixing models implemented in the SMOS L2 algorithm were used, i.e., the Dobson model for most soil types (Dobson et al., 1985) and the Mätzler model in the special case of very dry sandy soils (Matzler, 1998).

The transmissivity of the vegetation layer γ_P is calculated from the vegetation optical depth τ_P by taking into account the variation in vegetation slant height with angle as:

$$\gamma_P(\vartheta) = \exp(-\tau_P(\vartheta) / \cos\vartheta). \tag{2}$$

In L-MEB a sophisticated modelling approach is used to account for the effect of the vegetation structure on the dependence of the τ_P on polarisation and incidence angle. The value of optical depth τ_P at a particular incidence angle is expressed as a function of the value of τ_P at nadir (τ_{NAD}) as in:

$$\tau_P(\vartheta) = \tau_{NAD}\left(cos^2\vartheta + tt_P * sin^2\vartheta\right), \tag{3}$$

where tt_V and tt_H are empirical vegetation structure parameters that correct the optical depth for non-nadir views at each polarisation. A value of $tt_P>1$ or $tt_P<1$ will correspond, respectively, to an increasing or decreasing trend of τ as a function of the incidence angle ϑ. The nadir value of the vegetation optical depth τ_{NAD} (independent of both incidence angle and polarisation) can then be related to the vegetation water content (VWC) or, for global applications, the vegetation LAI, using empirical relationships, commonly using a linear relationship based on a land cover specific parameter b for VWC (Jackson et al., 1982) and b',b'' for LAI (Wigneron et al., 2007).

The reflectivity (Γ_P) of a rough surface is modelled in L-MEB using a formulation based on Choudhury et al. (1979):

$$\Gamma_P(\vartheta) = \Gamma_P^*(\vartheta) \exp\left(-H_R(\vartheta)\, cos^{N_{RP}}\vartheta\right), \tag{4}$$

where H_R is a height parameter accounting for the surface roughness (related to the standard deviation of surface heights), and parameter N_{RP} accounts for the dependence of H_R on polarisation and view angle. The approach taken in the SMOS L2 algorithm was adopted in this study, with H_R modelled as a linear function to account for its observed dependence on soil moisture (CESBIO, 2011; Panciera et al., 2009b; Saleh et al., 2007)).

The quantity T_{EFF} in Eq. (1) accounts for the contribution of the soil temperature profile to the emission through:

$$T_{EFF} = T_{DEPTH} + (T_{SURF} - T_{DEPTH})^*(\theta / w_0) b_0, \tag{5}$$

where θ stands for the soil moisture content of the top 5 cm, T_{DEPTH} is the deep soil temperature (typically at 50 to 100 cm), T_{SURF} is the surface temperature (approximately corresponding to a depth interval of 0–5 cm), and w_0 and b_0 are semi-empirical parameters depending on the specific soil texture. In this study the values of $w_0 = 0.3$ m^3/m^3 and $b_0 = 0.3$ m^3/m^3, calibrated by De Rosnay et al., 2006; Wigneron et al., 2001), were used.

The L-MEB approach described so far was developed for moderately vegetated soils such as agricultural areas and prairies. In the case of forest, a few studies have demonstrated that contributions from the soil emission may still be appreciable at L-band (Grant, 2009; Ryu et al., 2007). Despite the complex attenuation/scattering mechanisms occurring in forest canopies, the zero-order τ–ω approach described so far has been adopted in this study for retrieval over the forested areas, for consistency with the methodology adopted by the SMOS L2 algorithm. It should be noted that in the case of forest the optical depth (τ_{FNAD}) and the scattering albedo have been shown to remain fairly constant with respect to polarisation, incidence angle and time. This is a result of the fact that branches, which are the main attenuation factor, generally present a strong variability in orientation (Della Vecchia et al., 2007; Ferrazzoli et al., 2002; Grant et al., 2007; Saleh et al., 2004).

2.2.2. Model validation and parameter selection

The L-MEB model has been specifically validated for the NAFE'05 study area using high-resolution (62.5 m) PLMR observations together with the detailed ground data on soil moisture, vegetation water content, and surface roughness collected at the 8 experimental farms (Panciera et al., 2009a). The retrieval accuracy was found to be better than 4.8%v/v for all crops and grasslands sites, when using a site specific, soil moisture dependent calibration of roughness parameter H_R. The soil moisture dependence of parameter H_R was supported by previous results (CESBIO, 2011; Saleh et al., 2007; Saleh et al., 2009) including an independent study made during the NAFE'05 experiment using the EMIRAD air-borne radiometer (Saleh et al., 2009). The values of all the other land cover-specific parameters required by the L-MEB model were set as the default values indicated in the SMOS ATBD (CESBIO, 2011). This set of parameters, including the H_R calibrated by Panciera et al. (2009a), was further verified in this study using 1 km PLMR observations collected over the 8 experimental farm. Results (not shown) indicated that soil moisture could be retrieved at 1 km resolution with an accuracy better than 6%v/v. Although high, these residual errors should be considered in light of the intrinsic imperfection of the ground measurements associated with random measurement error of the dielectric probe (not better than 3.3%v/v) and the random error associated with comparing point measurements with 62.5 or 1 km pixels due to the natural spatial variability of soil moisture. This can be well above 5%v/v even at local scale (Merlin et al., 2008).

Values of parameters τ_{FNAD}, ω, tt, N_R, and H_R for the Eucalypt forest in the study area were independently calibrated by Grant (2009), using airborne PLMR data collected during NAFE'05 for radiative transfer studies of forest over a small patch of forest in the south-eastern part of the study area. The study indicated that, after specific calibration of the forest optical depth and scattering albedo, soil moisture could be retrieved with an accuracy of 6%v/v across 8 days of observations. The values of the L-MEB parameters used throughout this study are summarised in Table 1.

2.3. High-resolution soil moisture maps

High-resolution (1 km) soil moisture maps of the entire NAFE'05 study area, to be used as soil moisture validation data sets for the analysis conducted throughout this study, were derived from the dual-polarised T_B observations collected during Regional flights. Despite the residual errors, observed in the soil moisture retrieved at 1 km resolution (see previous section), it was deemed adequate to utilise the high-resolution maps as soil moisture validation data sets given their comprehensive spatial coverage, which was crucial in this study given the need to validate coarse-pixel retrieval.

Consequently, soil moisture and optical depths were estimated using a 2-parameter inversion of the L-MEB model, using the land-cover-specific parameters described in Table 1. Given the relatively small spatial resolution (1 km), each pixel was assumed to be uniform. This simplification is justified given that the fields in the

Table 1
L-MEB surface type parameters for the main vegetation covers in the study area. θ is soil moisture. (*) the value of optical depth adopted is shown instead of that of parameter b.

Surface type	H_R	Q_R	N_{RH}	N_{RV}	tt_H	tt_V	ω_H	ω_V	b
Crop (wheat and barley)	1.6–1.1 × θ	0	0	−1	1	8	0	0	0.08
Native Grass	1.3–1.13 × θ	0	1	0	1	1	0	0.05	0.12
Forest	0.12		0	0	0.46	0.46	0.07	0.07	0.57*

$w_0 = 0.3$ m^3/m^3 and $b_0 = 0.3$ m^3/m^3 were used for all land cover types.

study area are mainly larger than 500 m × 500 m. Over forested pixels, retrieval of both soil moisture and vegetation optical depth may be highly inaccurate, depending on the density of the canopy (i.e., the vegetation optical depth). It was therefore decided to constrain the retrieval by imposing the value of the vegetation optical depth calibrated with the detailed forest study by Grant (2009), and to retrieve soil moisture only. This is expected to yield a better soil moisture retrieval accuracy than the case in which retrieval of both soil moisture and vegetation optical depth was attempted over the forest (Parde et al., 2004; Piles et al., 2010).

Ancillary information on land cover type, and soil and vegetation temperature are required for the inversion of L-MEB. Land cover across the study area was characterised by supervised classification of a 30 m resolution Landsat 5 Thematic Mapper scene acquired on October 21. Maps of soil texture for the study area were produced using soil particle size analysis performed on 88 soil samples (7 cm in diameter, 5 cm deep) collected at 2 km spacing uniformly across the study area, interpolated to the 1 km reference grid using an inverse distance technique. The soils in the study area were mostly loams (38% of samples), followed by equal proportions of sandy loams and clay loams, more frequent respectively in the southern part and north-eastern part of the study area.

Values for the soil temperatures at 2.5 cm and 15 cm were derived from the continuous soil temperature measurements at the eighteen permanent sites operating across the study area. Due to the lack of soil temperature measurements deeper than 15 cm, the assumption was made that the temperature at 15 cm depth is a good estimate of that at 50 cm required for the calculation of T_{EFF} in Eq. (5). Given the early time of regional flight acquisition, spatial temperature variation across the study area was small (less than 1.5 K at 2.5 cm and 15 cm, as recorded at the monitoring sites). A spatially uniform value of soil temperature was therefore assumed in the retrievals for both depths, taken as the average soil temperature between the monitoring sites at the reference time to which the T_B observations were normalised for soil temperature change (8:00 AM). The values of the canopy and 2.5 cm soil temperature were also assumed to be in equilibrium, in line with previous soil moisture studies (Jackson et al., 1999; Njoku et al., 2002).

The four maps of L-MEB retrieved soil moisture and vegetation optical depth for the NAFE'05 study area are shown in Fig. 2. Wet conditions on October 31 and November 7 were associated with the heavy rainstorms at the beginning of the experiment. Little or no rainfall was recorded throughout the rest of the experiment, and accordingly drier soil moisture conditions can be seen for November 14 and 21. During this drydown period, the southern part of the study area, which is characterised by a low flat plateau with sandstone-derived soils, dried more quickly than the northern part, characterised by steeper hills and black clay soils. The forested area in the southern part of the study area (see Fig. 1) exhibited drier conditions than the rest, whilst the cropped areas in the north-western part of the study area, maintained wetter conditions throughout the month.

2.4. Soil moisture retrieval approaches

The three retrieval approaches used in this study are described below, and their main characteristics summarised in Table 2. Each approach was used to retrieve soil moisture from the coarse-resolution dual-polarised T_B observations (5–40 km) produced by

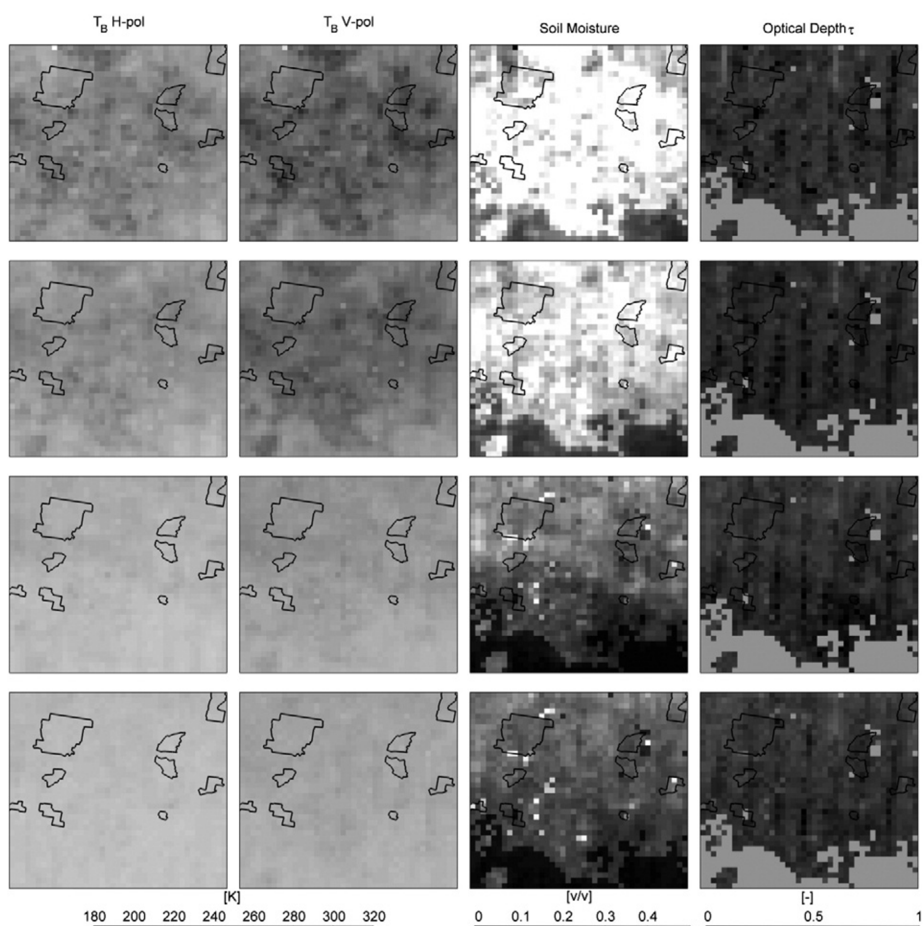

Fig. 2. Spatial maps of 1 km resolution PLMR brightness temperatures and L-MEB retrieved soil moisture and vegetation optical depth for the 40 km × 40 km NAFE'05 study area. Black polygons indicate the boundaries of the experimental farms.

Table 2
Main characteristics of the retrieval approaches tested. θ = soil moisture, τ = optical depth. Subscripts indicate that the parameter is retrieved for the entire pixel (pixel), moderate vegetation fraction (mod) or forest fraction (for). Parameters not indicated are set *a priori*.

Retrieval approach	Forward model	Retrieved parameters	*A priori* parameters	Main assumptions
Uniform pixel	Dominant land cover type only	θ_{pixel}, τ_{pixel}	–	• θ and τ uniform
SMOS approach	Each land cover type separately	θ_{pixel}, τ_{pixel}	–	• θ and τ uniform
Proposed extension	Each land cover type separately	θ_{pixel}, τ_{mod}	τ_{for}	• θ uniform

aggregation of airborne data. The error in soil moisture retrieval was assessed by comparing the coarse-resolution retrieved soil moisture with the average of the high-resolution soil moisture maps within each coarse pixel (hereby referred to as the "observed soil moisture"). The metrics used to assess the performance of the different approaches are those suggested in the SMOS L2 algorithm validation plan (CESBIO, 2006): that is, the Root Mean Square Error (RMSE) and bias between retrieved soil moisture and the average of the soil moisture validation data set, the latter being the arithmetic average of the high-resolution soil moisture maps described in Section 2.3 within each coarse pixel. For each land surface variable considered in the analysis, the standard deviation of the value of the quantity within the coarse pixel was used to characterise the magnitude of the variable's sub-pixel heterogeneity. The only exception was the land cover for which the magnitude of sub-pixel heterogeneity was characterised using the % cover of the pixel of the different land cover types.

2.4.1. Uniform pixel approach

The first approach tested in this study is a traditional uniform pixel approach. This approach was used to identify the land surface factors whose heterogeneity has the greatest impact on the soil moisture retrieval, as well as to quantify the error in soil moisture retrieval induced by such heterogeneity. The approach consists of inverting the L-MEB model to retrieve soil moisture and vegetation optical depth under the assumption that the pixel is uniform in terms of land cover, soil texture, soil temperature, canopy temperature and surface roughness. The L-MEB parameters used in the retrieval are those associated to the dominant land cover type of the pixel. Values of the L-MEB ancillary data for each coarse-resolution pixel are calculated by averaging the spatially distributed values of each land surface factor within the coarse pixel.

2.4.2. The SMOS retrieval approach

The second approach tested in this study is the soil moisture retrieval scheme implemented in the SMOS L2 processor (referred to here as "the SMOS retrieval approach"), and described in detail in the SMOS ATBD (CESBIO, 2011). The approach consists of applying L-MEB in forward mode separately for each land cover type present in the pixel to simulate fraction-specific T_B's, which are then aggregated based on the pixel fraction occupied to give a weighted-average pixel T_B. These land cover fractions are determined using high-resolution thematic maps. One or two parameters are then retrieved (a pixel average soil moisture, or a pixel average soil moisture and optical depth, depending on the quality and quantity of available concurrent observations). When the optical depth of the forest fraction present in the pixel is expected to be low (as is the case for the Eucalypt forest in the NAFE'05 study area, due to sparsely distributed trees), the retrieved parameters are considered to be the same in each sub-pixel land cover fractions, whilst all other parameters input of L-MEB model are land-cover-specific (grassland, forest and crop). According to the Global Forest Resources Assessment (FRA 2000) of the Food and Agricultural Organization (FAO), forest with canopy density similar to that of the Eucalypt woodland in the study area (30–60% density) represent 8% of the total land mass.

Given the nature of the NAFE'05 study area, this study is limited to the "nominal" case of the SMOS L2 algorithm, i.e., when either the low to moderately vegetated soil or the forest land cover classes are dominant within the SMOS field of view. Therefore, when running L-MEB in this study the forward model is applied separately to the grassland, forest and crop fractions of the footprint.

Since the focus of this study is to test the core fractional coverage approach implemented in SMOS L2, and not the whole processor, some simplifications were made which should be considered before extending the results of this study to an operational SMOS context: (i) the coarse-resolution observations were considered free of the errors associated with image reconstruction, ionospheric (Faraday) rotation and sky and atmospheric contributions compensation which are estimated to amount to a combined error of 0.5 K (CESBIO, 2011); and (ii) the radiometric uncertainty considered was that of the PLMR radiometer (2 K and 0.7 K respectively at V and H polarisation), which is lower than that estimated for SMOS (3.5 K at boresight and 5.8 K within 32° from boresight (McMullan et al., 2008). As the radiometric uncertainty is expected to be the main contributor to the error budget, the findings of this study should therefore be considered a best-case scenario of SMOS operational retrieval.

2.4.3. Proposed extension to the SMOS approach

An extension to the SMOS approach is proposed which accounts for the heterogeneity in vegetation optical depth within the SMOS pixel. This proposed extension is similar to the SMOS approach described in the previous section in that it uses a fractional forward modelling approach to retrieve one value for each free parameter (soil moisture and optical depth) considered uniform across the pixel. However, in the proposed extension the optical depth of the forest fraction is assumed *a priori* in the forward modelling. Consequently, the retrieved optical depth corresponds only to that of the moderate vegetation fraction (grass or crop). The proposed extension is therefore expected to provide a more accurate retrieval than the SMOS approach, since the emissions of the various pixel fractions are modelled using more realistic values of optical depth than in the case of the SMOS approach.

3. Results

The strategy utilised in the following sections was that of initially analysing the coarse-scale retrieval using the uniform pixel retrieval scheme alone, in order to identify the land surface factors whose heterogeneity have the greatest impact on the soil moisture retrieval and to quantify the error in soil moisture retrieval when such heterogeneity is not accounted for. The SMOS retrieval approach and the proposed extension are then analysed and their performance compared with the uniform pixel approach.

3.1. Effect of land surface heterogeneity in mixed forest and moderate vegetation pixels

The effect of land surface heterogeneity on coarse-scale soil moisture retrieval was analysed in the case of pixels with mixed forest and moderate vegetation biomass using the uniform pixel retrieval approach. In Fig. 3 the soil moisture retrieved from the coarse T_B observations is compared with the observed soil moisture. For easy visualisation, only 5, 20 and 40 km resolutions are displayed in the figure; the complete error statistics including all resolutions analysed can be found in Table 3. Whilst in Fig. 3 there is a good agreement between retrieved soil moisture at all resolutions and soil moisture conditions, there are many examples of pixels having errors higher than the SMOS target accuracy (4%v/v). The errors tended to be greater in wet conditions and were characterised by overestimation of

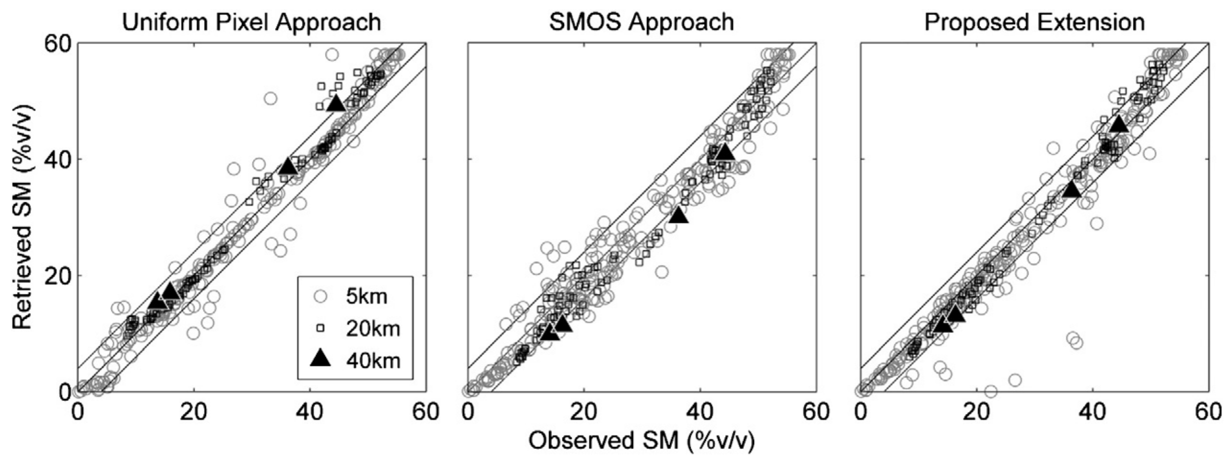

Fig. 3. Performance of the soil moisture retrieval at various resolution using the approaches tested in this study: uniform pixel approach (left panel), the current SMOS baseline algorithm (middle panel) and the proposed extension to the SMOS approach (right panel). The observed soil moisture corresponds to the soil moisture maps derived from 1 km airborne observations. Black Lines indicate the SMOS target accuracy (±4%v/v).

the pixel average soil moisture. It is also notable that as the resolution became coarser, the retrieval was more accurate (RMSE decreased from 3.1%v/v at 5 km to 2.6%v/v at 30 km resolution) but the distribution of the error tended to be positively biassed.

In Fig. 4 the retrieval error using the uniform pixel approach is compared with the sub-pixel heterogeneity of land cover type, soil moisture, vegetation optical depth and soil texture for each 5 km pixel. The effect of heterogeneity in soil temperature was not included in this plot, given the small spatial variability observed at the continuous monitoring sites across the study area. The effect of the heterogeneity in surface roughness, although not explicitly shown in Fig. 4, is implicitly included in the effect of land cover heterogeneity, since the surface roughness parameter in L-MEB is land cover specific. Fig. 4 shows that a significant correlation existed between the soil moisture retrieval error and the variability of land cover type within the pixel. In particular, a strong correlation was observed between the retrieval error and the fraction of the pixel occupied by native grass and forest (panels e and f). Panel f shows that the retrieval errors were below SMOS target accuracy for very low forest fraction (i.e., pixels mostly occupied by native grass and a small amount of crops). However, as the forest fraction increased the retrieval error increased as well, exceeding the SMOS target accuracy when the forest fraction was above approximately 30% and achieving a maximum error (overestimation) of 17.2%v/v when the forest fraction was approximately 50%. A further increase in forest fraction produced a strong discontinuity in the error, which exhibited an underestimation (−10%v/v) that decreased quickly until falling below the SMOS target accuracy again when the pixel was mostly occupied by forest. This difference in the sign of the error is a consequence of the fact that the uniform pixel approach considers the pixel to be uniformly occupied by the land cove type having the highest fraction of the pixel. Therefore, two pixels presenting similar cover fractions (*e.g.*, fractions of grass and forest close to 50%) will be modelled with very different parameters (those of grass or forest), depending on the predominance of either land cover type, resulting in the strong discontinuity in the error sign observed. As a result, the pixel average soil moisture is overestimated when a pixel containing a significant amount of forest is modelled as having a uniform native grass cover and underestimated when the same pixel is modelled as having a uniform forest cover. These results show that, as a result of the heterogeneity in land cover, the algorithm distorts the value of the free parameters (in this case soil moisture and optical depth) in order to match the simulated pixel microwave emission to that observed. Since the pixel emission-soil moisture curve is not linearly related to the different emission-soil moisture curves of the various pixel sub-fractions, the retrieved soil moisture differs from the true pixel-average soil moisture.

Panels a and b in Fig. 4 suggest a potential impact of the sub-pixel heterogeneity of soil moisture and vegetation optical depth on the

Table 3
Soil moisture error statistics obtained for the study period with all the approaches tested in this study at each resolution of observation. The best results for each resolution and group of pixels are indicated in underlined bold. All values are in %v/v soil moisture content.

Pixel resolution (No. of pixels)	Approach	All pixels		Pixel type A forest<40%		Pixel type B forest 40–60%		Pixel type C forest>60%	
		RMSE	Bias	RMSE	Bias	RMSE	Bias	RMSE	Bias
5 km *(254)*	Uniform pixel	3.1	0.2	1.8	0.3	7.7	2.0	3.2	−2.0
	SMOS approach	5.2	−2.6	4.0	−1.0	4.1	−3.1	1.9	−1.2
	Proposed extension	4.4	−1.0	2.6	−0.3	2.8	−0.3	1.8	0.4
10 km *(196)*	Uniform pixel	3.0	0.1	2.2	0.7	7.0	−2.1	4.7	−4.2
	SMOS approach	4.3	−2.0	3.5	−1.2	4.2	−3.7	3.2	−2.6
	Proposed extension	3.2	−0.7	2.4	−0.3	2.8	−0.5	2.0	0.0
20 km *(100)*	Uniform pixel	2.7	1.3	2.7	1.3	–	–	–	–
	SMOS approach	3.1	−1.8	3.1	−1.8	–	–	–	–
	Proposed extension	2.5	−0.3	2.5	−0.3	–	–	–	–
30 km *(36)*	Uniform pixel	2.6	1.5	2.6	1.5	–	–	–	–
	SMOS approach	3.1	−2.6	3.1	−2.6	–	–	–	–
	Proposed extension	2.4	−0.6	2.4	−0.6	–	–	–	–
40 km *(4)*	Uniform pixel	3.1	2.5	3.1	2.5	–	–	–	–
	SMOS approach	4.9	−4.8	4.9	−4.8	–	–	–	–
	Proposed extension	2.5	−1.7	2.5	−1.7	–	–	–	–

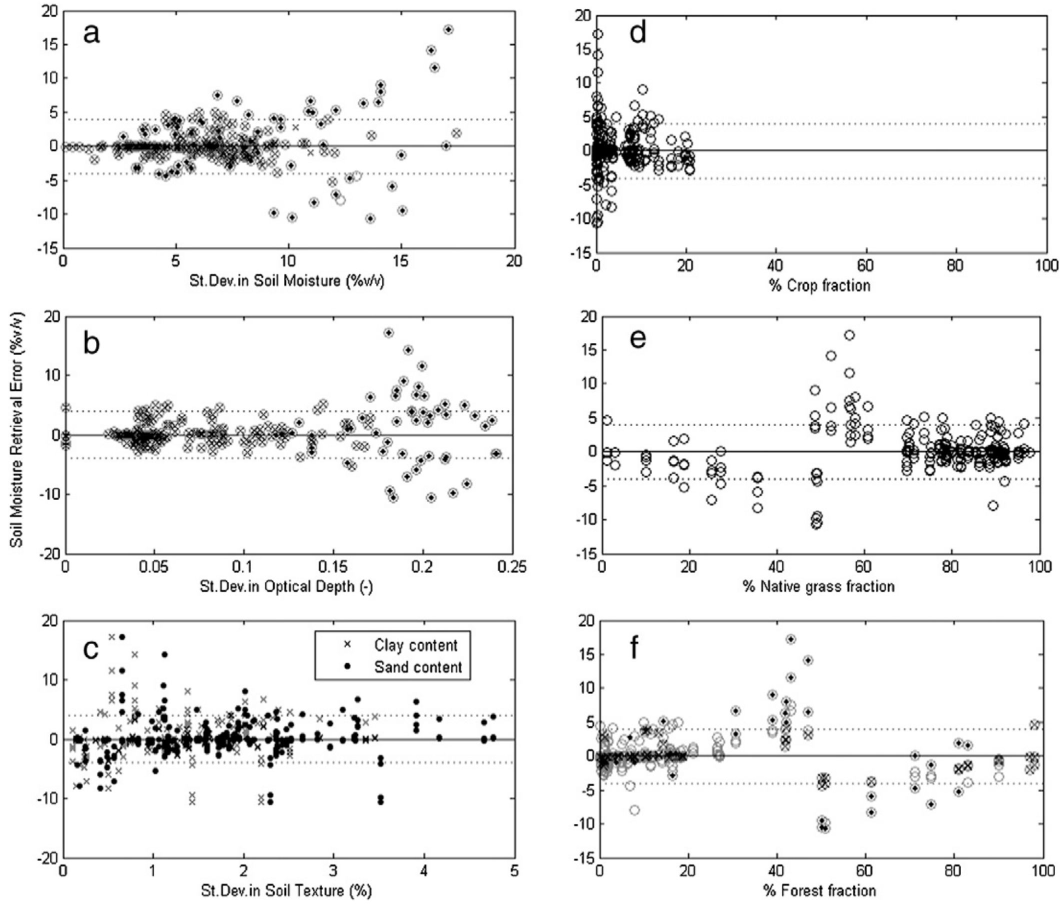

Fig. 4. Relationship between soil moisture retrieval error at 5 km resolution using the uniform pixel approach and the sub-pixel heterogeneity of (a) soil moisture, (b) vegetation optical depth, (c) clay and sand content and pixel fraction of crop, (d) crop, (e) native grass, and (f) forest. In panel (a) and (b), pixels with forest fraction between 25% and 75% (black dots) and forest fraction smaller than 25% or larger than 75% (crosses) are highlighted. In panel (f), pixels with soil moisture standard deviation larger than 10%v/v (black dots) and smaller than 5% (crosses) are highlighted. Dashed horizontal lines indicate the soil moisture target accuracy (±4%v/v).

retrieval error, with larger errors associated with elevated standard deviation of soil moisture and optical depth within the pixel. However, a detailed comparison with panel f reveals that this is only an indirect effect of the correlation between soil moisture distribution and optical depth and the land cover type itself. This is highlighted in panels a and b where data points with almost uniform land cover (forest fraction smaller than 25% or greater than 75%) are highlighted with crosses, showing that no correlation was observed between the retrieval error and the soil moisture or optical depth heterogeneity in these conditions. In both panels a and b the high retrieval errors are associated instead with heterogenous land cover conditions (black dots). Conversely, in panel f an increase in forest fraction caused an increase of the retrieval error for both uniform soil moisture (crosses, soil moisture standard deviation smaller than 5%v/v) and heterogeneous soil moisture conditions (black dots, soil moisture standard deviation larger than 10%v/v). No significant correlation was observed between the retrieval error and the sub-pixel heterogeneity of percentage of clay and sand content (panel c), with the highest errors at low standard deviations being clearly an artefact of the large number of pixels having low standard deviation of soil texture.

The analysis conducted thus far with pixels having relatively fine resolution (5 km) allowed consideration of the largest possible variety of land cover conditions within the NAFE'05 study area. The extrapolation of these results to coarser resolutions is subject to understanding whether the critical land cover conditions seen to produce the higher retrieval errors (~50% native grass and ~50% forest fraction) also occur at coarser resolutions. This in turn is subject to the presence of patches of forest and native grass large enough to occupy at least 50% of the pixels at coarser resolutions. To verify this, Table 4 shows the maximum sub-pixel fraction for each land cover type calculated amongst all the pixels analysed at each resolution (note that the crop, native grass, and forest fractions do not necessarily amount to 100%, as they may correspond to different pixels). Table 4 indicates that, since the NAFE'05 study area is largely occupied by native grass, the maximum fraction of pixel occupied by forest (hence the occurrence of pixels with the critical conditions of land cover heterogeneity) decreases substantially from 5 km to 40 km resolution. This resolution dependency is reflected in the decreasing of maximum retrieval error, also shown in Table 4. In order to work out whether the retrieval error produced by the critical conditions of land cover heterogeneity at the 40 km resolution is comparable to that observed

Table 4
Resolution dependence of the maximum sub-pixel fractions of each land cover type (columns 1–3), maximum soil moisture errors obtained using the uniform pixel approach for all pixels (column 4) and for pixels with fractions similar to those of the 40 km pixel (column 5). (*) Pixels with approximately 73% grassland, 22% forest and 4.6% crop, with number of pixels satisfying the criteria indicated in brackets.

Pixel resolution	(1) Native grass %	(2) Forest %	(3) Crop %	Maximum retrieval error (%v/v)	
				(4) All pixels	(5) Selected pixels*
5 km	97.8	98.2	20.9	+17.2	+6.6 (48)
10 km	94.4	70.0	17.3	+12.2	+7.3 (48)
20 km	90.2	38.5	11.0	+10.6	+6.7 (24)
30 km	85.8	25.1	7.4	+7.2	+7.2 (24)
40 km	73.0*	22.1*	4.6*	+5.5	+5.5 (4)

at 5 km resolution, the error for pixels with land cover fractions similar to those of the 40 km pixels (73.0% native grass, 22.1% forest and 4.6% crop) were extracted for each resolution (rightmost column in Table 4). Note that this error was calculated using the uniform pixel approach. The retrieval error for this subset of pixels was very similar at all the resolutions, varying by less than 1.1%v/v from 5 km to 40 km sized pixels, confirming that the effect of the heterogeneity of land cover is invariant with resolution. Given the limited number of 40 km resolution pixels available for this study, it was not possible with this dataset to generalise this conclusion on the resolution-invariance of the error due to land cover heterogeneity. However, the results presented in Table 4 show that this conclusion holds for the NAFE'05 study area. It follows that, were the critical conditions of land cover heterogeneity observed for a 40 km resolution pixel, with all other factors remaining constant, the soil moisture retrieval error could be as high as that observed at 5 km resolution,. It should be noted that the correlation of the retrieval error with the fraction of crops within the pixel could not be properly analysed in the present study, since the maximum percentage of crop fraction was quite small (20%) even for the finest resolution pixels.

3.2. SMOS retrieval approach

In this section the SMOS retrieval approach is tested in order to assess the ability of the approach to account for the sub-pixel heterogeneity of land cover, which in the previous section was shown to produce a significant error in soil moisture retrieval under a uniform pixel assumption. The performance of the SMOS approach as compared with the uniform pixel approach is shown in Fig. 3 for three resolutions (5, 20 and 40 km). At 5 km resolution, the SMOS approach significantly reduced the large errors obtained using the uniform pixel approach. However, at coarser resolution (20–40 km) the uniform pixel approach gave overall better results than the SMOS approach. As anticipated earlier, this apparent discrepancy is due to the fact that the NAFE'05 study area is mainly occupied by native grass, and therefore the heterogeneity decreases as the resolution decreases, being far from the critical conditions of land cover heterogeneity (~50% native grass and ~50% forest fraction).

To overcome this problem and assess in detail the performance of the SMOS approach, Table 3 shows the error metrics of the comparison between SMOS approach and uniform pixel approach for various resolutions. The pixels were here grouped according to the forest fraction (the remaining part of the pixel being occupied by grassland and crop in some cases): In group A, pixels are occupied predominantly by moderate vegetation (forest fraction<40%); group B contains heterogeneous pixels with land cover conditions shown in Section 3.1 to be critical for the retrieval (forest fraction between 40 and 60%); whilst group C contains pixels occupied predominantly by forest (forest fraction>60%). The SMOS approach significantly reduced the soil moisture RMSE on all dates in the case of heterogeneous type B pixels, with a decrease from 7.7%v/v (uniform pixel) to 4.1%v/v. (SMOS approach). Despite the efficacy of the SMOS approach on type B pixels, the approach exhibited a dry bias (underestimation), which is notable in Table 3 for both type A (−1%v/v) and type B pixels (−3.1%v/v). Moreover, in type A pixels this bias was accompanied by a high RMSE, which increased from 1.8%v/v when using the uniform pixel approach to 4.0%v/v when using the SMOS approach. These results suggest that the fractional forward modelling scheme of the SMOS approach is an improvement over the uniform pixel approach in pixels characterised by an approximately equal fraction of forest and moderately vegetated soil, where the heterogeneous land cover determines high retrieval errors under the assumption of pixel uniformity. However, in the case of pixels mostly occupied by moderately vegetated soil (crop or grassland) and a small amount of forest, the SMOS approach is less accurate than a simple uniform pixel approach, introducing in particular a dry bias.

In order to investigate the origin of this bias, the performance of the SMOS approach was analysed in detail for type A pixels in terms of the sub-pixel land cover fractions of grassland, crop and forest. The results (not shown) indicate that for pixels mainly occupied by grassland (>90%), the SMOS approach provided retrieval errors comparable to that of the uniform pixel approach. This was true even when a relatively small fraction of the pixel was occupied by another moderate vegetation land surface type (crop in this case). However, in the presence of even a small fraction of forest in a pixel otherwise occupied by grassland, the SMOS approach led to the bias observed in Table 3. Based on these observations, it is argued that the SMOS approach will lead to underestimation of the pixel-average soil moisture as a result of retrieving a single value of optical depth (assumed to represent the entire pixel), in pixels characterised by a strong contrast between the radiative transfer properties of forest areas and moderately vegetated areas, such as grassland or crops. This happens because a lower soil moisture value is needed for the algorithm to find the right balance between the modelled emissions of the various pixel fractions under the constraint, imposed by the SMOS approach, of uniform optical depth and soil moisture between the pixel fractions.

3.3. Proposed extension to the SMOS approach

The extension to the SMOS approach proposed in this study accounts for the heterogeneity in vegetation optical depth within the SMOS pixel by imposing the optical depth of the forest fraction *a priori* in the forward modelling, whilst retrieving only the optical depth of the moderate vegetation fraction (grass and/or crop). The performance of the proposed extension is compared to that of the other approaches tested in Fig. 3 and Table 3. It was initially assumed in the analysis that the optical depth of the forest fraction is known accurately, and was consequently set to the value specifically obtained over the NAFE'05 Eucalypt forest (0.57, J. Grant pers. comm.). The impact of uncertainties in this *a priori* information is analysed at the end of this section. Table 3 shows that the proposed extension led to an improvement of the soil moisture retrieval accuracy with respect to the other approaches for pixels of types B and C, with the dry bias which affected the SMOS approach being reduced to −0.3%v/v and the RMSE to 2.8%v/v.

Interestingly, the uniform approach was the more accurate of the approaches tested on uniform and moderately vegetated pixels (type A) at 5 km resolution, due to the negative bias discussed in Section 3.2 affecting both the SMOS approach and the proposed extension. This was further analysed using synthetic scenarios where the methods were applied assuming exact knowledge of all the ancillary data, including the radiative transfer parameters. The results (not shown) confirmed that this negative bias persisted, suggesting that it is a direct effect of the fractional forward modeling due to the non-linearities of the radiative transfer equations. However, the bias is of second-order with respect to the impact of sub-pixel heterogeneity, explaining why on heterogeneous type B pixels the SMOS approach and extended approach were more accurate than the uniform approach (as they compensated for the first-order effect of heterogeneity), whilst on type A pixels the two methods were less accurate than the uniform approach (as both methods were affected by the second-order bias). These results suggest that on uniform land cover conditions a fractional modelling approach would constitute little or no advantage over a simple uniform pixel approach.

The analysis is extended in Table 3 to all available resolutions. It should be noted that, given the nature of the NAFE'05 study area (22% forest fraction, 4.6% crops and 73% grassland), all pixels with resolution coarser than 10 km were fairly uniform type A pixels. Nevertheless, the main observations drawn from the analysis at 5 km resolution held well at coarser resolutions. In particular, that the SMOS approach partially reduced the error due to the heterogeneity of land cover in heterogeneous group B and forested group C pixels at 10 km. However, the dry soil moisture bias continued to affect the SMOS approach at such coarser resolutions. Consequently, the proposed extension provided the most accurate soil moisture retrieval in heterogeneous group B and forested group C pixels at 5–10 km resolutions. It is important to highlight that the accuracy of the proposed extension was substantially constant across resolutions (with only an increase in dry bias, not exceeding −1.4%v/v), whereas that of the uniform pixel approach degraded significantly as the resolution became coarser (overall RMSE for the study period increasing from 1.8%v/v to 3.1%v/v). As a result, the proposed extension was more accurate than the uniform pixel approach in pixels at resolutions coarser than 10 km, in contrast with what observed at 5–10 km resolutions. These results also suggest that, although the analysis in the case of groups B and C land cover conditions was limited to resolutions finer than 10 km resolutions, the proposed extension should be more accurate were such land surface conditions observed at resolutions more typical of SMOS.

The proposed extension requires as input an *a priori* estimate of the forest optical depth. In a SMOS operational context, such estimates will be derived by empirical relationships with ancillary maps of LAI, which themselves will be subjected to uncertainties (CESBIO, 2011). It is therefore important to assess how the assumption made in this study, that the forest optical depth is known accurately, might impact the results. This was tested by creating 4 random sets of optical depth values, all normally distributed around the correct value (0.57) but with different standard deviations (0.1, 0.2, 0.3 and 0.4). A set of 100 random *a priori* values of forest optical depth was created for each standard deviation and soil moisture was estimated for each 5 km NAFE'05 observation using the proposed approach. The results, shown in Fig. 5, indicate that the accuracy of the *a priori* information on the optical depth of forest had a significant impact in heterogeneous group B pixels, with a strong increase in RMSE observed as the uncertainty about the optical depth of forest increased. However, the proposed extension was more accurate than the SMOS approach for an optical depth uncertainty up to 0.2, which corresponds to an error of 35%v/v. Conversely, the accuracy of the *a priori* information on optical depth had little impact on the soil moisture retrieval for more uniform moderately vegetated pixels (group A). In this case, the RMSE using the proposed extension was only slightly degraded (by 0.4%v/v). In pixels mostly covered by forest (Group C), the accuracy of the proposed extension degraded quickly with increasing optical depth uncertainty, as expected. It should be noted that whilst the SMOS and uniform pixel approaches led to significant soil moisture biases in group B and C pixels, the proposed extension approach was able to provide more accurate results even in the case of strong uncertainty in the value of the forest optical depth (70%).

Exact figures on the accuracy of the estimation of the forest optical depth by means of ancillary LAI data do not currently exist, particularly for Eucalyptus forests. This is mainly because, differently than soil moisture, the vegetation optical depth is not a directly measurable physical quantity. Therefore its accuracy is typically determined indirectly, through the accuracy of the forest emission modelled using a particular value of optical depth. However, recent studies have shown that MODIS LAI products can achieve an accuracy of 0.5 for forest sites (Wang et al., 2004). A recent review of the forward modelling approach used in SMOS to derive the forest optical depth from LAI data (Ferrazzoli, P., pers. comm.) indicates that this uncertainty would translate to an uncertainty of forest optical depth of 0.1, which is better than the uncertainty of 0.2 allowed in this assessment.

4. Conclusions

The fractional coverage forward modelling approach that is core to the SMOS L2 processor was assessed using extensive airborne L-band data over pixels composed of a mix of Eucalypt forest and vegetation pixels with moderate biomass, for varying degrees of soil moisture, soil texture and vegetation water content heterogeneity. Subsequently an extension to the SMOS approach was proposed and shown to improve the soil moisture retrieval accuracy over heterogeneous pixels at the

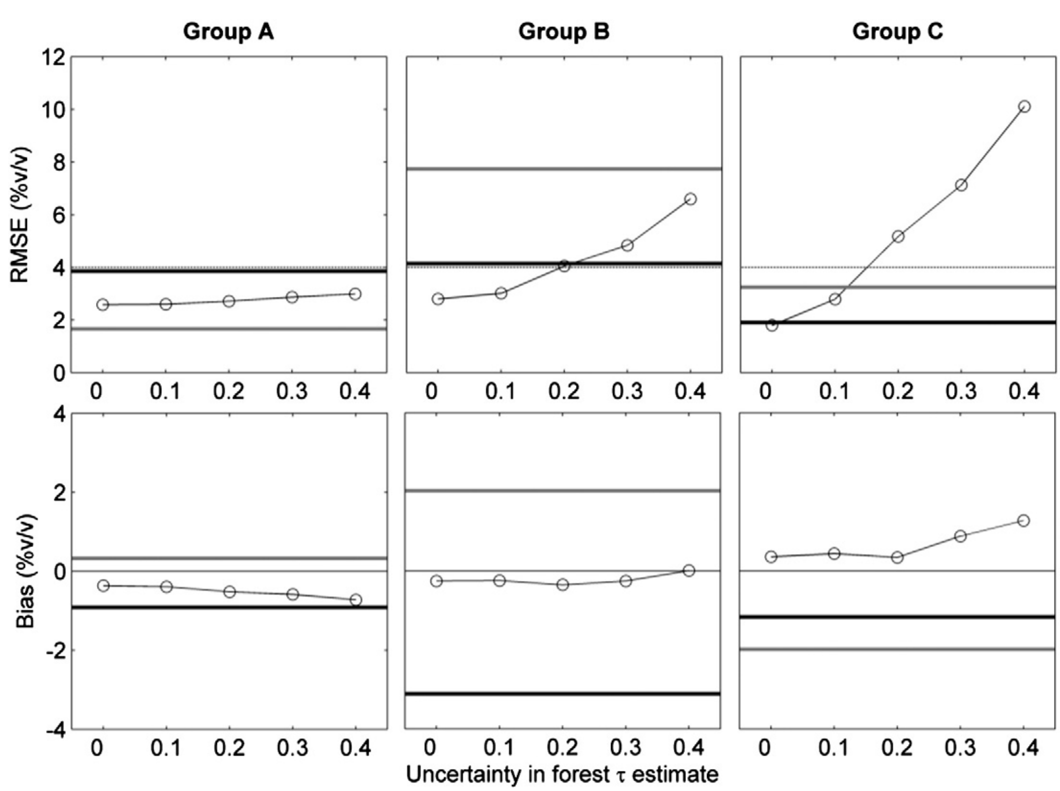

Fig. 5. Impact of uncertainty in the *a priori* information on the forest optical depth on the soil moisture retrieval error using the proposed extension to the SMOS retrieval approach (circles), for pixels of group A (forest fraction<40%, left column), group B (forest fraction = 40–60%, middle column) and group C (forest fraction>60%, right column). Also shown are the errors obtained using the current SMOS baseline algorithm (thick black line) and the uniform pixel approach (thick grey line).

limited cost of needing a crude estimate of the forest optical depth. Using a uniform pixel retrieval approach it was first shown that a significant correlation existed between the soil moisture retrieval error and the sub-pixel heterogeneity of land cover type. Whilst accurate retrievals were obtained in uniform vegetated pixel of moderate biomass (grassland and crop) the error was significant when the pixel was composed by 50% grassland and 50% forest fraction, with an overall soil moisture RMSE for the study period of 7.7%v/v (with 2%v/v bias) for pixels with 40-60% forest fraction.

The fractional coverage modelling approach adopted by SMOS was shown to provide more accurate retrievals in the case of pixels with 40–60% forest; the overall RMSE for the study period was reduced from 7.7%v/v to 4.1%v/v. However, the SMOS approach was shown to be less accurate than a uniform pixel approach in the case of uniform, moderately vegetated pixels (grassland and crop) with a modest forest fraction (less than 40%). In these cases the overall soil moisture RMSE was increased from 1.8%v/v to 4.0%v/v. Moreover, the soil moisture retrieval using the SMOS approach suffered from a dry bias.

An extension to the SMOS approach was proposed which relaxes the assumption of uniform optical depth between the modelled pixel fractions, by imposing the optical depth of forest and retrieving only the optical depth of the moderately vegetated fraction together with a uniform soil moisture value for the pixel. The proposed extension significantly improved the retrieval accuracy for the particular combination of land covers in the study area; in heterogeneous pixels presenting a 40–60% forest fraction, the overall soil moisture RMSE for the study period decreased from 4.1%v/v to 2.8%v/v. The dry bias was also reduced from −3.1%v/v to −0.3%v/v. It was also shown that the proposed approach provides better soil moisture estimates than the SMOS baseline approach even with a crude estimate of the optical depth of forest, corresponding to a 35% relative uncertainty. Therefore, it is expected that sufficiently accurate estimates of the optical depth of forest at L-band could be derived from routinely available global maps of LAI in order to implement the approach proposed in this study in a SMOS operational context.

Given the limited extent of cropping in the NAFE'05 study area, the results of this study have been limited to pixels characterised mainly a mix of forest and grassland. Further analysis is needed to assess whether the proposed extension would be efficient in pixels with large portions of mature crops (such as in intensive irrigation areas in south-eastern Australia and certain parts of the USA). Moreover, the approach should be tested with the SMOS data, which was not available at the time when this study was conducted.

Acknowledgements

The National Airborne Field Experiment 2005 was made possible through infrastructure (LE0453434) and research (DP0557543) funding from the Australian Research Council, and the collaboration of a large number of scientists from throughout Australia, United States and Europe. The authors wish to thank Phillip Maisongrande and Gilles Boulet at the Centre d'Etudes Spatiales de la BIOsphere (CESBIO) for the supervised classification of the Landsat 5 Thematic Mapper scene, and Cristina Martinez for providing the laser mastersizer soil particle analysis data.

References

Bindlish, R., & Barros, A. P. (2002). Subpixel variability of remotely sensed soil moisture: An inter-comparison study of SAR and ESTAR. *IEEE Transactions on Geoscience and Remote Sensing*, *40*(2), 326–337.

Bolten, J. D., Crow, W. T., Jackson, T. J., Zhan, X., & Reynolds, C. A. (2010). Evaluating the utility of remotely-sensed soil moisture retrievals for operational agricultural drought monitoring. *IEEE Journal of Selected Topics in Applied Earth Observations and Remote Sensing*, *3*, 57–66.

Burke, E. J., Shuttleworth, W. J., & Houser, P. R. (2004). Impact of horizontal and vertical heterogeneities on retrievals using multiangle microwave brightness temperature data. *IEEE Transactions on Geoscience and Remote Sensing*, *42*(7), 1495.

Burke, E. J., & Simmonds, L. P. (2003). Effects of sub-pixel heterogeneity on the retrieval of soil moisture from passive microwave radiometry. *International Journal of Remote Sensing*, *24*(10), 2085–2104.

Castillo, V. M., Gómez-Plaza, A., & Martínez-Mena, M. (2003). The role of antecedent soil water content in the runoff response of semiarid catchments: A simulation approach. *Journal of Hydrology*, *284*(1–4), 114–130.

CESBIO (2006). *Algorithm validation plan for SMOS L2 SMPPD.* Technical Report. Centre d'Etudes Spatiales de la BIOsphère Available online at. www.cesbio.ups-tlse.fr/data_all/SMOS-doc/CBSA/L2-SM_algovalP_V015_1g.pdf

CESBIO (2011). *Algorithm theoretical basis document (ATBD) for the SMOS level 2 soil moisture processor development continuation project, issue 3.4.* Technical Report. Centre d'Etudes Spatiales de la BIOsphère Available Online at. http://www.cesbio.ups-tlse.fr/data_all/SMOS-doc/atbd/ATBD_v3_4_20110124.pdf

Choudhury, B. J., Schmugge, T. J., Chang, A., & Newton, R. W. (1979). Effect of surface-roughness on the microwave emission from soils. *Journal of Geophysical Research-Oceans and Atmospheres*, *84*(Nc9), 5699–5706.

Conil, S., Douville, H., & Tyteca, S. (2007). The relative influence of soil moisture and SST in climate predictability explored within ensembles of AMIP type experiments. *Climate Dynamics*, *28*, 125–145.

Davenport, I. J., Sandells, M. J., & Gurney, R. J. (2008). The effects of scene heterogeneity on soil moisture retrieval from passive microwave data. *Advances in Water Resources*, *31*(11), 1494–1502.

De Rosnay, P., Calvet, J. -C., Kerr, Y., Wigneron, J. -P., Lemaitre, F., Escorihuela, M. J., et al. (2006). SMOSREX: A long term field campaign experiment for soil moisture and land surface processes remote sensing. *Remote Sensing of Environment*, *102*(3–4), 377–389.

Della Vecchia, A., Ferrazzoli, P., Wigneron, J. P., & Grant, J. P. A. G. J. P. (2007). Modeling forest emissivity at L-band and a comparison with multitemporal measurements. *IEEE Geoscience and Remote Sensing Letters*, *4*(4), 508–512.

Dobson, M. C., Ulaby, F. T., Hallikainen, M. T., & El-Rayes, M. A. (1985). Microwave dielectric behavior of wet soil-part II: Dielectric mixing models. *IEEE Transactions on Geoscience and Remote Sensing*, *GE-23*(1), 35–46.

Drusch, D., Wood, E. F., & Simmer, S. (1999). Up-scaling effects in passive microwave remote sensing: ESTAR 1.4 GHz measurements during SGP '97. *Geophysical Research Letters*, *26*(7), 879–882.

Ferrazzoli, P., Guerriero, L., & Wigneron, J. P. (2002). Simulating L-band emission of forests in view of future satellite applications. *IEEE Transactions on Geoscience and Remote Sensing*, *40*(12), 2700–2708.

Galantowicz, J. F., Entekhabi, D., & Njoku, E. G. (2000). Estimation of soil-type heterogeneity effects in the retrieval of soil moisture from radiobrightness. *IEEE Transactions on Geoscience and Remote Sensing*, *38*(1), 312–316.

Grant, J. P. (2009). Measurement and modelling of L-band forest emission for future soil moisture retrieval from SMOS signatures, PhD Thesis, Vrije Universiteit Amsterdam.

Grant, J. P., Wigneron, J. P., Van de Griend, A. A., Kruszewski, A., Sobjaerg, S. S., & Skou, N. (2007). A field experiment on microwave forest radiometry: L-band signal behaviour for varying conditions of surface wetness. *Remote Sensing of Environment*, *109*(1), 10–19.

Guha, A., & Lakshmi, V. (2002). Sensitivity, spatial heterogeneity, and scaling of C-band microwave brightness temperatures for land hydrology studies. *IEEE Transactions on Geoscience and Remote Sensing*, *40*(12), 2626–2635.

Jackson, T. J. (2001). Multiple resolution analysis of L-band brightness temperature for soil moisture. *IEEE Transactions on Geoscience and Remote Sensing*, *39*(1), 151–164.

Jackson, T. J., Le Vine, D. M., Hsu, A. Y., Oldak, A., Starks, P. J., Swift, C. T., et al. (1999). Soil moisture mapping at regional scales using microwave radiometry: The Southern Great Plains Hydrology Experiment. *IEEE Transactions on Geoscience and Remote Sensing*, *37*(5), 2136–2151.

Jackson, T. J., Schmugge, T. J., & Wang, J. R. (1982). Passive microwave sensing of soil-moisture under vegetation canopies. *Water Resources Research*, *18*(4), 1137–1142.

Kerr, Y., & Njoku, E. G. (1993). On the use of passive microwaves at 37 GHz in remote sensing of vegetation. *International Journal of Remote Sensing*, *14*, 1931–1943.

Koster, R. D., Suarez, M. J., Higgins, R. W., & Van den Dool, H. M. (2003). Observational evidence that soil moisture variations affect precipitation. *Geophysical Research Letters*, *30*(5).

Matzler, C. (1998). Microwave permittivity of dry sand. *IEEE Transactions on Geoscience and Remote Sensing*, *36*(1), 317–319.

McMullan, K. D., Brown, M. A., Martin-Neira, M., Rits, W., Ekholm, S., Marti, J., et al. (2008). SMOS: The payload. *Geoscience and Remote Sensing, IEEE Transactions on*, *46*(3), 594–605.

Merlin, O., Walker, J. P., Kalma, J. D., Kim, E. J., Hacker, J., Panciera, R., et al. (2008). The NAFE'06 data set: Towards soil moisture retrieval at intermediate resolution. *Advances in Water Resources*, *31*(11), 1444–1455.

Merlin, O., Walker, J., Panciera, R., Young, R., Kalma, J., & Kim, E. (2007). *Soil moisture measurement in heterogeneous terrain.* International Congress on Modelling and Simulation (MODSIM). New Zealand: Christchurch.

Njoku, E. G., Hook, S. J., & Chehbouni, A. (1996). Effects of surface heterogeneity on thermal remote sensing of land parameters. In E. T. E. J. B. Stewart, R. A. Feddes, & Y. Kerr (Eds.), *Scaling up in hydrology using remote sensing* (pp. 19–39). New York: Wiley.

Njoku, E. G., Wilson, W. J., Yueh, S. H., Dinardo, S. J., Li, F. K., Jackson, T. J., et al. (2002). Observations of soil moisture using a passive and active low-frequency microwave airborne sensor during SGP99. *IEEE Transactions on Geoscience and Remote Sensing*, *40*(12), 2659–2673.

Panciera, R. (2009). Effect of Land Surface Heterogeneity on Satellite Near- Surface Soil Moisture Observations. Civil and Environmental engineering. Melbourne, University of Melbourne. PhD.

Panciera, R., Walker, J. P., Kalma, J. D., Kim, E. J., Hacker, J., Merlin, O., et al. (2008). The NAFE'05/CoSMOS data set: Towards SMOS soil moisture retrieval, downscaling and assimilation. *IEEE Transactions on Geoscience and Remote Sensing*, *46*(3), 736–745.

Panciera, R., Walker, J. P., Kalma, J. D., Kim, E. J., Saleh, K., & Wigneron, J. P. (2009a). Evaluation of the SMOS L-MEB passive microwave soil moisture retrieval algorithm. *Remote Sensing of Environment*, *113*(2), 435–444.

Panciera, R., Walker, J. P., & Merlin, O. (2009b). Improved understanding of soil surface roughness parameterization for L-band passive microwave soil moisture retrieval. *Geoscience and Remote Sensing Letters, IEEE*, *6*(4), 625–629.

Panciera, R., Walker, J. P., Kim, E., Kalma, J., & Merlin, O. (2007). *Effect of spatial scale on soil moisture retrieval from passive microwave sensors.*

Parde, M., Wigneron, J. P., Waldteufel, P., Kerr, Y. H., Chanzy, A., Sobjaerg, S. S., et al. (2004). N-parameter retrievals from L-band microwave observations acquired over a variety of crop fields. *Geoscience and Remote Sensing, IEEE Transactions on*, *42*(6), 1168–1178.

Piles, M., Vall-llossera, M., Camps, A., Talone, M., & Monerris, A. (2010). Analysis of a least-squares soil moisture retrieval algorithm from L-band passive observations. *Remote Sensing*, *2*(1), 352–374.

Ryu, D., Jackson, T. J., Bindlish, R., & Le Vine, D. M. (2007). L-band microwave observations over land surface using a two-dimensional synthetic aperture radiometer. *Geophysical Research Letters*, *34*(L14401).

Saleh, K., Kerr, Y. H., Richaume, P., Escorihuela, M. J., Panciera, R., Delwart, S., et al. (2009). Soil moisture retrievals at L-band using a two-step inversion approach (COSMOS/NAFE'05 experiment). *Remote Sensing of Environment*, *113*(6), 1304–1312.

Saleh, K., Wigneron, J. P., Calvet, J. C., Lopez-Baeza, E., Ferrazzoli, P., Berger, M., et al. (2004). The EuroSTARRS airborne campaign in support of the SMOS mission: First results over land surfaces. *International Journal of Remote Sensing*, *25*(1), 177–194.

Saleh, K., Wigneron, J. -P., de Rosnay, P., Calvet, J. -C., Escorihuela, M. J., Kerr, Y., et al. (2006). Impact of rain interception by vegetation and mulch on the L-band emission of natural grass. *Remote Sensing of Environment*, *101*(1), 127–139.

Saleh, K., Wigneron, J. P., Waldteufel, P., de Rosnay, P., Schwank, M., Calvet, J. C., et al. (2007). Estimates of surface soil moisture under grass covers using L-band radiometry. *Remote Sensing of Environment*, *109*(1), 42–53.

Uitdewilligen, D. C. A., Kustas, W. P., & van Oevelen, P. J. (2003). Estimating surface soil moisture with the scanning low frequency microwave radiometer (SLFMR) during the Southern Great Plains 1997 (SGP97) hydrology experiment. *Physics and Chemistry of the Earth, Parts A/B/C*, *28*(1–3), 41–51.

Van de Griend, A. A., Wigneron, J. P., & Waldteufel, P. (2003). Consequences of surface heterogeneity for parameter retrieval from 1.4-GHz multiangle SMOS observations. *IEEE Transactions on Geoscience and Remote Sensing*, *41*(4), 803.

Wang, Y., Woodcock, C. E., Buermann, W., Stenberg, P., Voipio, P., Smolander, H., et al. (2004). Evaluation of the MODIS LAI algorithm at a coniferous forest site in Finland. *Remote Sensing of Environment*, *91*(1), 114–127.

Western, A. W., Zhou, S. L., Grayson, R. B., McMahon, T. A., Bloschl, G., & Wilson, D. J. (2004). Spatial correlation of soil moisture in small catchments and its relationship to dominant spatial hydrological processes. *Journal of Hydrology*, *286*(1–4), 113–134.

Wigneron, J. P., Kerr, Y., Waldteufel, P., Saleh, K., Escorihuela, M. J., Richaume, P., et al. (2007). L-band microwave emission of the biosphere (L-MEB) model: Description and calibration against experimental data sets over crop fields. *Remote Sensing of Environment*, *107*(4), 639–655.

Wigneron, J. P., Laguerre, L., & Kerr, Y. H. (2001). A simple parameterization of the L-band microwave emission from rough agricultural soils. *IEEE Transactions on Geoscience and Remote Sensing*, *39*(8), 1697–1707.

Wigneron, J. P., Waldteufel, P., Chanzy, A., Calvet, J. C., & Kerr, Y. (2000). Two-dimensional microwave interferometer retrieval capabilities over land surfaces (SMOS mission). *Remote Sensing of Environment*, *73*(3), 270–282.